RSC Advances

PAPER

View Article Online
View Journal | View Issue

Cite this: *RSC Adv.*, 2018, **8**, 37872

Ascorbic acid sensor using a PVA/laccase-Au-NPs/Pt electrode

Yuan-Gee Lee,[a] Bo-Xuan Liao[b] and Yu-Ching Weng *[b]

A surface-modified electrode, PVA/laccase-Au-NPs/Pt, was prepared to sense ascorbic acid (H_2A) in this study. An amount of the following composite, PVA/laccase-Au-NPs/Pt, the polyvinyl acetate (PVA) was employed as a surfactant to adhere the substrate, Pt; then the laccase peptides were spun inside the PVA fiber to wind around the immobilized Au-NPs and construct a hierarchical structure. The PVA shell layer was in charge of sensing H_2A and transmitting electrical signals, *i.e.* transducing redox reaction of H_2A. Inside the core region, laccase peptides were responsible for transducing electrons and the Au-NPs collected and relayed them to the substrate of the Pt electrode. It was found that the sensing mechanism for the transducing laccase molecules involved a long-chain electron transmission and peroxide bridging, and for the sensed object, H_2A, is related to a sequential discharge of two electrons. According to a test of the catalytic activity, the sensitivity increased with the increase of the doped Au-NPs up to a maximum amount and then decreased because excess Au-NPs tended to agglomerate and obstruct the relaying electrons. The response time and sensitivity were measured to be *ca.* 40 s and 1.8 μA cm^{-2} ppm. The surface-modified electrode, PVA/laccase-Au-NPs/Pt, was found to show good selectivity among several disturbing reagents and good stability for 76 days.

Received 25th July 2018
Accepted 30th October 2018

DOI: 10.1039/c8ra06280c

rsc.li/rsc-advances

Introduction

To date, ascorbic acid (H_2A), also known as vitamin C, has received increasing attention because it is indispensable for humans. An insufficient supply of H_2A in the body can cause symptoms such as scurvy, but an excess supply of H_2A results in stomach convulsions. In addition to this, H_2A helps in promoting healthy cell development, normal tissue growth, and repairs and heals injuries and burns.

Ascorbic acid is difficult to measure directly because of its characteristics of being water soluble, antioxidant, and lack of storage in the body. Various H_2A sensors have been developed with many versatile functions and few advantages. Ion sensitive field effect transistors (ISFET) are highly stable with a quick response, but the lithography of the transistor structure costs are high.[1] Optical H_2A sensors can detect H_2A *in situ* without disturbances, but are constrained by environmental factors, *e.g.*, temperature and optical source.[2] Conductometric sensors can be operated with ease but have issues such as sensitivity, selectivity, and accuracy, which deviate considerably from an ideal sensor.[3] Potentiometric sensors prevailed at great odds in miniature working areas, but it's slow response and ionic noise are frustrating for operators.[4] Amperometric sensors overcome some of the disadvantages mentioned above. They are usually designed in a laminate structure, film/substrate, in which the film is proportionally sensitive to specific chemicals. The amperometric sensor possesses a wide range of detection concentrations and has a relatively fast response among H_2A sensors.[5]

Laccase, *p*-diphenol:dioxygen oxidoreductase, *i.e.* EC 1.10.3.2, is part of a large group of enzymes that catalyze organics with fast electron transfer mechanisms.[6] Laccase can be covalently immobilized on a platinum electrode to detect aromatic diamine, catechol, and catecholamines by substrate recycling.[7] However, the weak bond strength of bulk Pt–O and the small specific area of the modified electrode constrains its reliability and sensibility. To resolve this problem and improve reliability, we modified the surface of the electrode by introducing an electric mediator, *i.e.* Au-NPs, that effectively transfer electrons during a redox reaction.[8] The nanoscale Au manifests quantum effects that amplifies the sensing signal.[9] For resolving this problem, we employed laccase molecules to provide sites for the redox reactions of the H_2A molecules. On these reaction sites, laccase molecules electrocatalyzed the redox reaction of H_2A and transmitted the oxidizing current to the immobilized Au-NPs. Therefore, the laccase peptides can sense H_2A and transmit electrical signals to the signal-receiving Au-NPs that collect the transduced electrons and relay them to the substrate of the Pt electrode. The reason being that the bulk Au possesses a high surface energy, 1400 erg cm^{-1},[2] the Au-NPs tends to be wetted by the support, PVA with low surface energy of 36.5 erg cm^{-1},[2] or the spun laccase peptides. Therefore, the Au-NPs and the laccase peptide were firmly immobilized onto

[a]*Department of Automation Engineer, Institute of Mechatronoptic Systems, Chienkuo, Technology University, Taiwan. E-mail: yglee@ctu.edu.tw*

[b]*Department of Chemical Engineering, Feng Chia University, Taichung, Taiwan, 40724. E-mail: ycweng@fcu.edu.tw; Tel: +886-4-24517250; +886-4-24510890 ext. 3689*

the PVA ribbon and the Pt substrate. This paper characterizes the hierarchical structure using a scanning electron microscope (SEM) and explores the electrochemistry using a potentiostat to measure sensitivity, catalysis activity, and endurance.

Experimental

Preparation of modified PVA/laccase-Au-NPs/Pt electrode

Platinum slices with the following dimensions, 10 mm × 10 mm × 1 mm, were polished and cleaned with deionized water ultrasonically to be used as the substrate of the electrode. A batch of 7 wt% PVA solution was prepared as a stock solution by blending 7 g polyvinyl acetate (PVA), Sigma Fw: 14 600–18 600, in 93 ml of reverse osmosis (RO) water at 70 °C. After cooling to room temperature, 10 ml of the PVA stock solution was blended with different weight loading, 2, 4, 6, 8, 10, and 12 mg, of laccase, Sigma Co., and 0.025 g of Au-NPs, Lihochem Co. This blended laccase-PVA-Au-NPs solution was drawn into a syringe for injecting into the electro-spinning equipment, FES-COL Agent Wanted Co., with a flow speed of 0.08 ml min^{-1}. Before spinning, the wettability of the substrate surface was tested with a contact angle meter, Kyowa Face CA-D. The operation voltage and working distance were set to be 18 kV and 15 cm, respectively. After spinning the laccase-PVA-Au-NPs solution on to the substrate, the spun electrode was further sprayed with 5 wt% of H_2SO_4-contained glutaraldehyde to crosslink the PVA linkage for 15 min. The cross-linked electrode was subjected to a series of microstructural investigations, including SEM (3000 H Hitachi Co.), energy dispersive spectroscopy (Noran Voyager 2.0) and phase identification (D8-SSS Bruker Co.).

Preparation of the phosphate buffer solution, PBS, and tested chemicals for selectivity

A stock buffer solution was prepared by blending 14.2 g of Na_2HPO_4 and 12 g of NaH_2PO_4, Showa Co., in a 1000 ml flask. Hereafter, the pH value was adjusted by H_3PO_4 and NaOH, Showa Co. In addition, a batch of 1.419 M H_2A (Acros Co.) was stocked in a dark brown pipe for the selectivity test. A series of disturbance reagents were prepared for contrast including, 1.38 M glucose (Showa Co.); 1.3 M citric acid (Showa Co.); 1.43 M tartaric acid (Showa Co.); 1.43 M sucrose (Showa Co.); 1.43 M fructose (Acros Co.); 1.43 M oxalic acid (Showa Co.); and 3.375 mM uric acid (Alfa Aesar Co.). All the responses resulting from the reagents were compared with that of the ascorbic acid.

Qualitative and quantitative measurements for H_2A

Cyclic voltammetry with different scan rates was applied to investigate the characteristic redox peaks of H_2A. The obtained voltammograms were further analyzed to determine the voltage range for the redox limiting currents. After constructing a dependence of limiting curve *vs.* applied potential, the specific voltage for chrono-amperometry was determined to construct stable currents stepwise, which lead to a quantitative calibration curve. In addition, a successive response for stability test up to 78 days was obtained to ensure its reproducibility.

Results and discussion

Morphology investigation and phase identification of the electrode

The laccase peptides were found to immobilize on the Au-NPs that were embedded in the PVA fibers. Fig. 1(a) shows a smooth feature for electrodes that contain the Au-NPs inside the PVA fibers. Though the nanoscale Au particles were highly attracted to each other, no agglomeration as nodes were found. This suggests a homogeneous distribution for the Au-NPs inside the PVA ribbons. As laccase peptides joined the structure of the PVA ribbon, the PVA fibers still demonstrated a smooth feature (Fig. 1(b)). This is due to the low surface energy of organics in the PVA and the laccase molecules. The PVA was suitable for dewetting the laccase molecules with some remaining segregation. In contrast to the smooth features in Fig. 1(b), PVA was spun as an outer tube and the laccase peptides segregated inside the tube as a core shell.

The inner laccase molecules have to bind to each other since the peptides search for low activation energy to nucleate by adsorbing on some Au-NPs crystals, and this was measured qualitatively (Fig. 1(c)). Therefore, we can briefly conclude that the PVA ribbon embedded the laccase molecules, and they bonded as peptides winding around the Au-NPs.[10] Schön *et al.* performed analogous research in which an organic ligand shell surrounded a gold cluster to act like a dielectric "spacer" generating capacitances between neighbouring clusters down to 10 F.[11] In water-containing solutions, this ligand-surrounded cluster acted as quantum dots with a condensed state to show narrow and hopping bands. On the quantum dots, even though these Au-NPs were not interconnected, a single electron tunneling (SET) effect inspired the fast transduction of electrons in the circuit to transmit electrical signals during the charge/discharge processes. In a similar way, the laccase peptides provide immobilization sites for the Au-NPs that interconnect through the PVA fibers into a nanowire network in

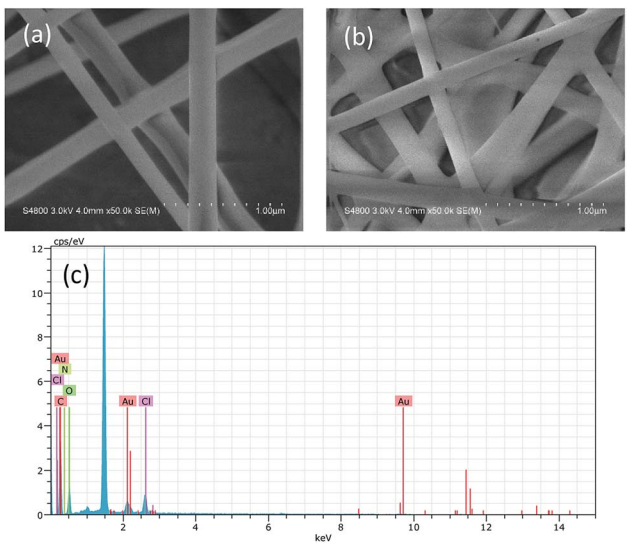

Fig. 1 Morphology of the electrodes. (a) PVA/Au-NPs/Pt and (b) PVA/laccase-Au-NPs/Pt as well as (c) the energy dispersive spectrum of (b).

charge of electron relay.[12] Fig. 2 illustrates the hierarchical graft of the PVA/laccase-Au-NPs/Pt electrode with a schematic plot.

The Au-NPs aligned inside the PVA fiber with a preferred orientation. Fig. 3 shows the X-ray diffraction patterns for the consequent modified electrodes. Except for the Au(111) peak, all three electrodes showed a similar pattern. The specific peak in the PVA/laccase-Au-NPs/Pt, *i.e.* Au(111), not only confirmed the existence of the Au-NPs, but also showed a sharp peak to induce texture (111). This confirms the former deduction regarding laccase peptides being apt to adsorb on some crystals, or, moreover, on a specific crystallographic orientation of the Au-NPs.

The Nyquist plot

The laccase-Au-NPs can reduce charge transfer resistance in the faradaic process. Fig. 4(a) shows the Nyquist plot for different electrodes, Pt, PVA/Pt, and PVA/laccase-Au-NPs/Pt as well as the analyzed model, Fig. 4(b). Note that the symbols in the inserted model, Randles equivalent circuit, were the solution resistance, R_Ω, connecting with parallel elements, including a double layer capacitance, C_d, and a charge transfer resistance, R_{ct}, in series with a Warburg impedance, Z_w.[13] After fitting this model, the Pt electrode showed a solution resistance of *ca.* 4 Ω and a charge transfer resistance of 1 Ω. As the PVA is spun on the Pt electrode, the solution remained at 4 Ω and the charge transfer resistance increased up to 6.5 Ω. This elucidates an inert role for the PVA layer that obstructed the transfer of the faradaic current but maintained the value of the solution resistance. Further, the solution resistance increased to an appreciable amount, 5 Ω, and the charge transfer resistance reduced to 2 Ω when the laccase-Au-NPs modified the electrode, *i.e.* the PVA/laccase-Au-NPs/Pt. This suggests that the laccase-Au-NPs dominated the charge transfer, *i.e.* the electrochemical reaction, excluding the PVA layer from the double layer. The resistance of the PVA layer was merged with that of the solution to present a higher resistance of 5 Ω. In the meantime, the electrochemistry was facilitated by the laccase-Au-NPs with a low charge transfer resistance of 2 Ω. The semi-circle and the straight tail represent the kinetic control and mass transfer control mechanisms, respectively.

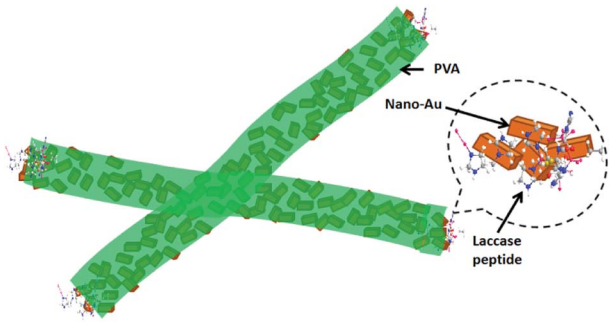

Fig. 2 A schematic plot of the hierarchical structure of the modified PVA/laccase-Au-NPs/Pt electrode.

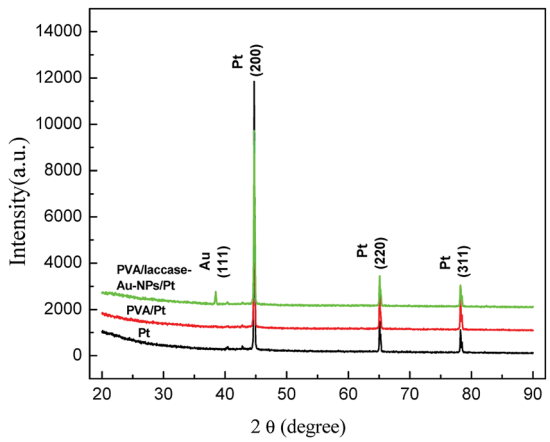

Fig. 3 X-ray diffraction patterns for different electrodes, Pt, PVA/Pt, and PVA/laccase-Au-NPs/Pt.

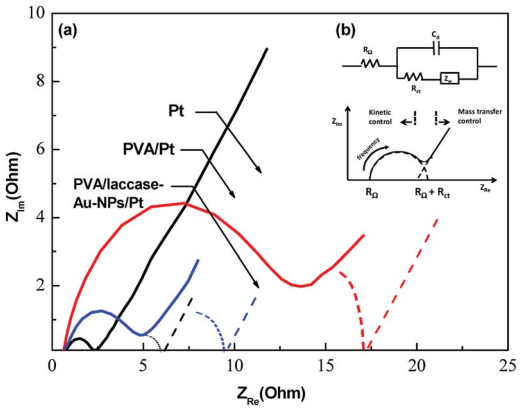

Fig. 4 (a) The impedance plot for the different electrodes with their extrapolations and (b) the analyzed model, Randles equivalent circuit. Note that the test solution, a buffer solution, contained 4 mM of H_2A inside.

We inferred that, according to the model in Fig. 4(b), the electrochemical reaction on the Pt electrode was kinetically controlled initially; and, after being covered with PVA, the PVA/Pt electrode became mass diffusion control. When the laccase-Au-NPs were joined and aligned inside the PVA fiber, the reaction mode transformed from mass transfer to kinetic control. This confirms the previous shell model hypothesis, in which the outer tube, PVA layer, acted as an inert layer to impede ion flow but the inner laccase-Au-NPs core was responsible for promoting the transfer. The charge transfer resistance, R_{ct}, was considerably reduced because the laccase could be in charge of sensing H_2A and transmitting electrical signals; and the wound Au-NPs serve as electrical circuits to reduce the charge transfer resistance in a faradaic process.

Cyclic voltammogram

The centers of the sp^3 hybrid orbital in the laccase molecules, T1, T2, and T3, are responsible for transduction in the cyclic charge/discharge processes. Fig. 5 shows the cyclic voltammograms for the different electrodes, Pt, PVA/Au-NPs/Pt, and PVA/

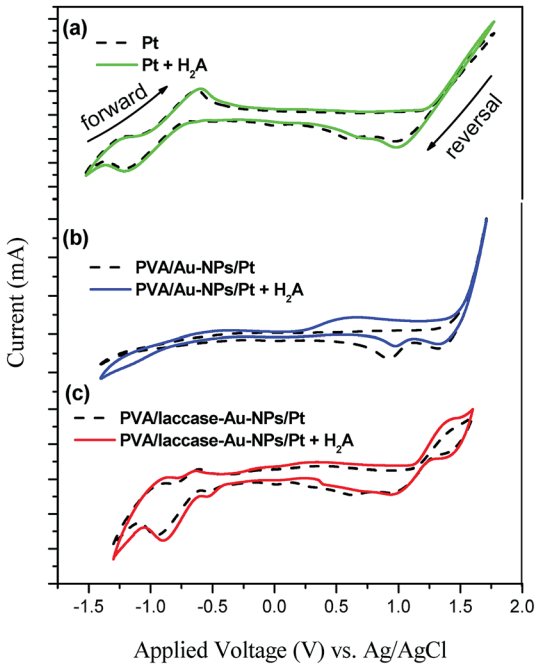

Fig. 5 Cyclic voltammograms to test the effects of 4 mM of H_2A, on the response current in the buffer solution for different electrodes, (a) Pt, (b) PVA/Au-NPs/Pt, and (c) PVA/laccase-Au-NPs/Pt.

laccase-Au-NPs/Pt, in both the blank solution without H_2A and the H_2A-containing solution. In Fig. 5(a), the two curves almost overlap and show no response current for the H_2A. In Fig. 5(b), strong reductive current peaks appear in the forward scan ranging from 0.25 V to 1.0 V; however, the immobilized Au-NPs tend to be leached from the spun PVA and therefore could not sustain the endurance test. Now, we focus on PVA/laccase-Au-NPs/Pt, which was superior for solutions both with and without H_2A. For the former voltammogram, the reductive current peaks appeared in the forward scan at −1.0 V and −0.7 V. The first peak is related to the adsorption/desorption process for the weakly bound hydrogen ions on the electrode, and the second peak can be related to the strong bonding between hydrogen and platinum.[14] Pitara *et al.* researched the behaviour of the adatoms on its preferred orientation and found that the first peak is prone to occur in the Pt(110) orientation and the second peak preferred the Pt(100) orientation.[15] This corresponds with the crystal type of the polycrystalline Pt substrate in the present electrode. With the increase of the voltage to a high voltage of 1.2 V, a strong peak stands out that represents the electrolysis of H_2O. In the reverse scan, two peaks appeared at 0.8 V and 0.6 V; they involve the discharge process of the laccase peptides that were composed of different ligand centers, T1, T2, and T3 (Fig. 6(a)).[16]

It is noteworthy that the T1 site of the laccase molecule is the primary electron acceptor either in solution, *i.e.* homogeneous case, or at the surface of the electrode, *i.e.* heterogeneous case.[17] The T1 site was confirmed to receive the electrons transferred from the adsorbed laccase enzyme with a close distance of 8 Å, which allows an efficient electron tunnelling through an internal electron transfer mechanism. For all the three centers, the electron transfer relies on the redox process between Cu(I) and Cu(II), which is expressed in the following[18]

$$Cu^{2+} + e^- \rightarrow Cu^+ \quad (1)$$

Because of different ligands, T2 and T3, immobilized on the Au-NPs[19] the released electron had to overcome a distinct energy barrier (Fig. 6(b)). In Procedure A, the charge transferred from T1 to T3. Though it involved a long-chain electron transmission, all the transmitting paths were amino groups with low energy barriers for the electron to proceed through. In Procedure B, in contrast, the transmitted electron not only passed across Procedure A, but it had to surmount a high energy barrier for peroxide bridging between T2 and T3.[20] This procedure takes longer time and requires activation at a high voltage. The applied voltage for the former procedure presented a low voltage, 0.6 V; and that for the latter procedure showed a high voltage, 0.8 V.

The Au-NPs supply the laccase peptide with adsorption sites and play the role of electron transfer mediator. This is due to the Au-NPs having appropriate dimensions and functionalization adjacent to the enzyme redox center, T1, T2 and T3. When the H_2A molecules undergo redox reactions to release electrons, the laccase peptide transduces the redox reaction and liberates electrons into the adsorption sites of the Au-NPs. The Au-NPs act as a current collector to relay these electrons onto the electrode preventing build-up. Moreover, the Au-NPs had the effect of aligning enzymes and electrically wiring redox-active centers to reduce the overpotential originating from the tunnelling barrier induced by the bridge spacer (Fig. 6(b)).[21]

When H_2A was blended, the response current varied considerably. On the reverse scan of the solid curve in Fig. 5(c), a broadened peak was found from 0.3 V to 1.0 V. This suggests

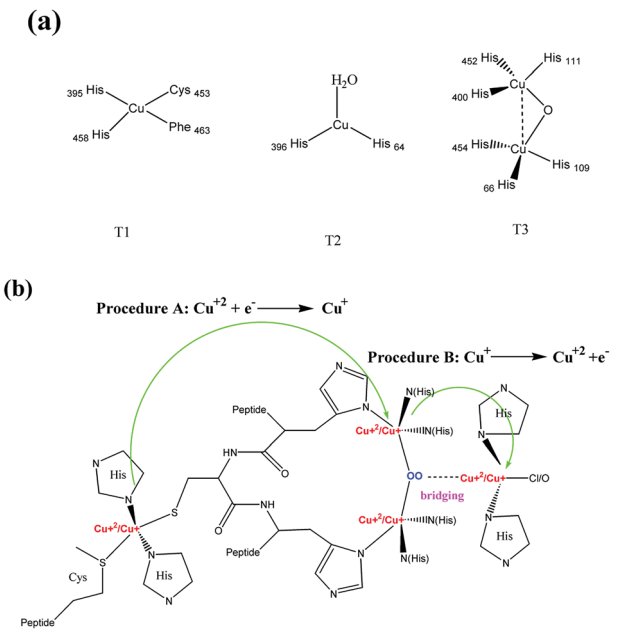

Fig. 6 (a) Three amino groups of laccase, T1, T2, and T3; and (b) the electron transfer pathways by peroxide bridging between T2 and T3.

the oxidation reactions of ascorbic acid to release electrons in the following manner

$$H_2A \rightarrow HA^+ + H^+ + e^- \quad (2)$$

$$HA^+ \rightarrow A^{2+} + H^+ + e^- \quad (3)$$

The first electron transfer in eqn (2) represented a serial oxidation process with a product, 2,3-diketogulonic acid (DKG); the second in eqn (3) is regarded as a sequential oxidation of the DKG.[22] Though the H_2A could release two electrons in both eqn (2) and (3), these two oxidation voltages were so close that the response current merged to give a plateau and covered over the response current resulting from the discharge of laccase. The laccase molecules were then responsible for the consequential signal conversion from chemical to electrical.[23] This is due to the specific role for laccase that received chemical signals and converted them into electrical signal. The laccase molecule played the role of a transducer here. In addition, it was found that the Au-NPs relayed the following electron transfer to prevent build-up. Therefore, the transmission of the sensing signal was facilitated by the Au nanoparticles.[24] Though the Au-NPs did not participate in H_2A-sensing, it acted as a mediator for fast charge transfer in the electrical circuit.

Polarization curve for H_2A detection

The polarization curves illustrate the detailed electrocatalysis mechanisms on the electrode. Fig. 7 shows the variation of the polarization current for both "no H_2A" and "H_2A containing". For the former, the response current increased with the applied voltage and approached a saturation voltage at 0.4 V. This suggests a discharge process to release electrons for oxidation reaction, *i.e.* from Cu(I) to Cu(II), at a low voltage range of less than 0.4 V. For the curve of "H_2A containing", the polarization curve shows two current ramps at voltages, −0.2 V to 0.0 V and 0.0 V to 0.4 V, which suggests two reaction mechanisms. At voltages from −0.2 V to 0.0 V, the oxidation of the laccase molecule still appears to show a ramp; however, the discharging of H_2A replaces the laccase oxidation to show another ramp at voltages from 0.0 V to 0.4 V.

Not only could the applied voltage detect H_2A with high sensitivity, but it also had to expel the disturbance resulting from other electrochemical reactions. To obtain high sensitivity, the applied voltage must be high enough to facilitate the discharge of the H_2A, *i.e.* larger than 0.2 V (Fig. 7); to prevent disturbances, the applied voltage was not allowed to be so high as to induce other electrochemical reactions. Therefore, the optimum applied voltage, 0.4 V, was determined by the next chronoamperometric test.

Chronoamperometric test

A linear calibration curve for H_2A was established in this study. Fig. 8(a) shows the variation of the response currents as a consequence of increasing the H_2A concentration. The response current grew stepwise with appreciable noise and the response time was measured at *ca.* 40 s. The stepwise response was plotted to fit with a linear relationship for a sensitivity of 1.8 μA cm^{-2} ppm, *i.e.* 52 μA cm^{-2} mM, (Fig. 8(b) inset). To compare with similar sensors for H_2A, Table 1 lists the electrodes and immobilization method for catalyst sensing. Uchiyama *et al.* employed an Au electrode with covalent binding to immobilize the catalyst. They achieved a sensitivity of 25.17 μA cm^{-2} ppm. In addition, they researched amperometric ascorbic acid sensors from enzyme micelle membranes, which obtained a higher sensitivity of 43.91 μA cm^{-2} ppm. However, this study prevailed over similar research. This is due to Au-NPs, which play a significant role during electrocatalysis. The catalysis activity was worthy of illustration in the following paragraph.

Au-NPs predominated the catalytic activity of the sensor for H_2A. Fig. 9 shows the sensitivity variation with different doped amount of the Au-NPs. The sensitivity increased with the increase of the doped amount up to a maximum and then decreased. This suggests that the larger the doped Au-NPs concentration, the more the transferred charge comes from the oxidation of H_2A. This confirms Hvolbæk and Haruta's research in which the active sites were located on the corners and edges of the Au nanoparticles.[31,32] The more Au-NPs and active sites have higher sensitivity for the electrode. However,

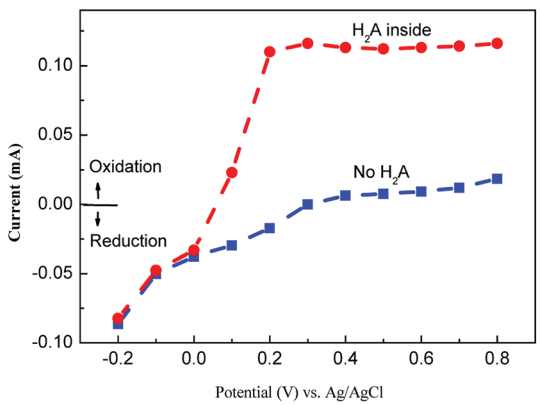

Fig. 7 Limiting current for both kinds of solutions, no ascorbic acid (no H_2A) and ascorbic acid containing (4 mM of H_2A inside) the buffer solution.

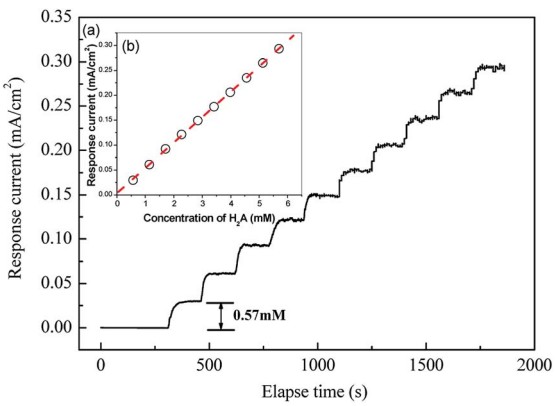

Fig. 8 (a) The response current of the modified electrode with different concentrations of H_2A in the buffer solution at the applied voltage 0.4 V *vs.* Ag/AgCl and the inset, (b) calibration curve.

Table 1 Comparison of different amperometric biosensor for H_2A

Electrode	Immobilized method	Applied potential (V) *vs.* Ag/AgCl	Sensitivity ($\mu A\ cm^{-2}\ mM^{-1}$)	H_2A conc. range (mM)	Ref.
Ascorbate oxidase					
Au	Cross-linking			5×10^{-4} to 1.2	25
AO-PEDOT-MWCNs/Pt disc	Electropolymerization		2.4	0.05–20	26
Au or AGCE	Covalent binding	AGCE			27
		−0.5	43.91	5×10^{-6} to 0.4	
		−0.3	25.17	0.01–0.6	
		Au			
		−0.7	9.77	0.01–0.6	
AO-GPTS/RuO2/C/Ag/Pc graphite/epoxy	Covalent binding dropped		13.85 mV mM^{-1}	0.02–1	28
			44 mV/pH 5.8	8×10^{-6} to 0.45	29
		0.4	44 mV/pH 5.8	8×10^{-6} to 0.45	30
Lacccase					
Laccase/CdTe/Cys/Au	Covalent binding	0.4	13.38	10×10^{-6} to 140	31
PVA/laccase-Au-NPs/Pt	Electro-spinning	0.4	52	0.57–5.7	This study

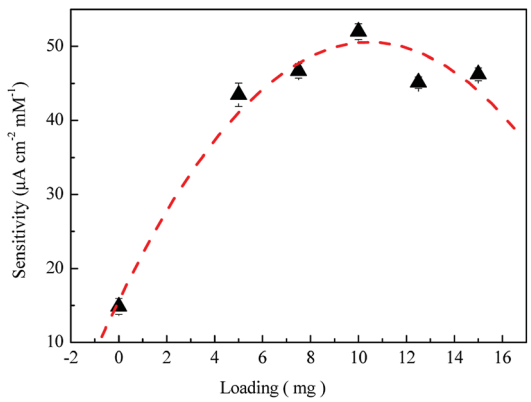

Fig. 9 The effect of Au-NPs for different weight loading, 2, 4, 6, 8, 10 and 12 mg, of laccase in spinning process on the sensitivity of the PVA/laccase-Au-NPs/Pt electrode in the buffer solution.

excess Au-NPs were prone to agglomeration, which could not collect the transduced electrons from the laccase molecule. Though the intimate contact between the Au-NPs lowered the interfacial charge resistance and substantiated a higher electrocatalytic response, the overall electrochemical performances were attributed to the synergistic effects of the laccase peptide catalyst and the Au-NPs electrical relay.[33]

Chemical selectivity of the ascorbic acid sensor

The laccase electrode, *i.e.* PVA/laccase-Au-NPs/Pt, demonstrated a highly selective sensing for H_2A. This is due to the general disturbance resulting from medical auxiliary reagents including glucose, fructose, sucrose, oxalic acid, citric acid, tartaric acid, and especially, uric acid, whose normal concentration in the human body ranges up to 8.3 mg dl^{-1}. Sequential reagent tests were performed to investigate its sensing selectivity, qualitatively. It was found that only H_2A showed a strong response and the others showed almost no current (Fig. 10).

Chemical reliability of the ascorbic acid sensor

The H_2A sensor was also stable. Fig. 11 shows sensitivity during a long sequential test. It is noteworthy that the sensitivity was

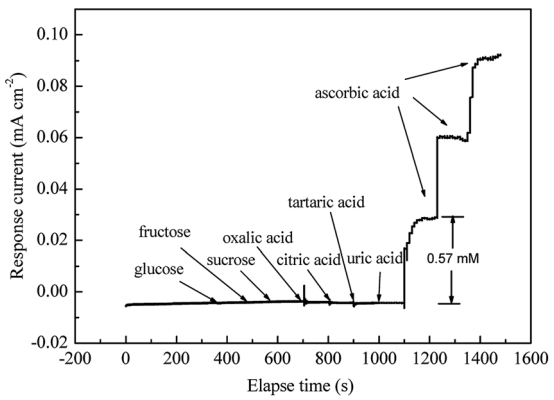

Fig. 10 Disturbance test with different disturbing reagents, glucose, fructose, sucrose, oxalic acid, citric acid, tartaric acid and uric acid in the buffer solution. Note that the applied voltage was kept at 0.4 V *vs.* Ag/AgCl.

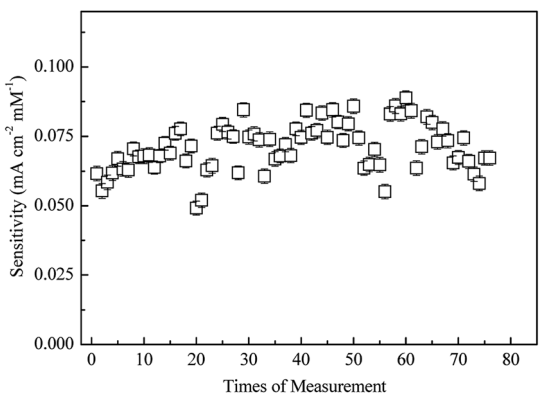

Fig. 11 Endurance of sensitivity for stability testing over 76 days. Note that the test solution contained 4 mM of H_2A inside the buffer solution.

measured sequentially for 76 days with a 4.3% standard deviation. This shows a good endurance in sensitivity for the modified electrode.

Conclusions

We prepared an electrode, PVA/laccase-Au-NPs/Pt, to sense H_2A. The hierarchy of PVA/laccase-Au-NPs showed a shell/core structure. Different layers were designed for distinct functions; the PVA shell layer was employed as a surfactant to adhere to the Pt substrate; the adsorbed laccase molecule was in charge of transducing the redox reaction to wind around the Au-NPs, which were responsible for electron transfer mediation. According to the Nyquist plot, PVA was inert for transferring current but the laccase-Au-NPs reduced the charge transfer resistance in a faradaic process. From the Randles equivalent circuit, kinetic control predominated the electrochemical charge transfer for the Pt electrode and after being covered with PVA, the PVA/Pt electrode became mass diffusion control. When the laccase-Au-NPs aligned inside the PVA fiber, the reaction mode transformed from mass transfer back to kinetic control.

From cyclic voltammograms, we found the charge/discharge mechanism for different ligands of the laccase molecule, T2 and T3, on Au-NPs induced distinct oxidation peaks resulting from the different energy barriers. When H_2A was blended, the response current appeared as a broadened peak from 0.3 V to 1.0 V because of a serial electron release from H_2A to A^{2-} ion. The optimum applied voltage for chronoamperometric measurement, 0.4 V *vs.* Ag/AgCl, was obtained by considering a high sensitivity to H_2A and with a minimal disturbance from other electrochemical reactions. A linear calibration curve for H_2A was established with a response time of *ca.* 40 seconds and a sensitivity of 1.8 μA cm^{-2} ppm. Additionally, the laccase electrode showed an exclusive sensitivity, *i.e.* selectivity, for H_2A among eight reagents that generally disturb the measurement of H_2A. This sensor also had a good endurance when tested sequentially over 76 days with 4.3% standard deviation.

Conflicts of interest

There are no conflicts to declare.

Acknowledgements

Support from the National Science Council of the Republic of China (MOST 106-2632-E-035-001) and Feng Chia University is gratefully appreciated. The authors also appreciate the Precision Instrument Support Center of Feng Chia University in providing the fabrication and measurement facilities.

Notes and references

1 S. Martinoia, G. Massobrio and L. Lorenzelli, *Sens. Actuators, B*, 2005, **105**, 14–15.
2 A. Jain, A. Chaurasia and K. K. Verma, *Talanta*, 1995, **42**, 779–787.
3 S. Ivanow, V. Tsakova and V. M. Mirsky, *Electrochem. Commun.*, 2006, **8**, 643–646.
4 M. K. Amini, S. SHahrokhian, S. Tangestaninejad and V. Mirkhani, *Anal. Biochem.*, 2001, **290**, 277–282.
5 M. Arvand, S. Sohrabnezhad and M. F. Mousavi, *Anal. Chim. Acta*, 2003, **491**, 193–201.
6 S. K. Lee, S. D. George, W. E. Antholine, B. Hedman, K. O. Hodgson and E. I. Solomon, *J. Am. Chem. Soc.*, 2002, **124**, 6180–6193.
7 D. Quan and W. Shin, *Electroanalysis*, 2004, **16**, 1576–1582.
8 B. Chalmer, *Physical Metallurgy*, John Wliey & Sons, New York, 1959.
9 V. Krikstolaityte, A. Barrantes, A. Ramanavicius, T. Arnebrant, S. Shleev and T. Ruzgas, *Bioelectrochemistry*, 2014, **95**, 1–6.
10 M. S. EI-Deab and T. Ohsaka, *Electrochem. Commun.*, 2007, **9**, 651–656.
11 G. Schön and U. Simon, *Colloid Polym. Sci.*, 1995, **273**, 101–117.
12 M. S. Hsu, Y. L. Chen, C. Y. Lee and H. T. Chiu, *ACS Appl. Mater. Interfaces*, 2012, **4**, 5570–5575.
13 J. E. B. Randles, *Discuss. Faraday Soc.*, 1947, **1**, 11–19.
14 J. J. Ruiz, A. Aldaz and M. Dominguez, *Can. J. Chem.*, 1978, **56**, 1533–1537.
15 E. L. Pitara and J. Barbier, *Appl. Catal., A*, 1997, **149**, 49–87.
16 S. Riva, *Trends Biotechnol.*, 2006, **24**, 219–226.
17 S. Shleev, A. Jarosz-Wilkolazka, A. Khalunina, O. Morozova, A. Yaropolov, T. Ruzgasd and L. Gorton, *Bioelectrochemistry*, 2005, **67**, 115–124.
18 H. B. Gray and J. R. Winkler, *Q. Rev. Biophys.*, 2003, **36**, 341–372.
19 S. V. Shleev, O. V. Morozova, O. V. Nikitina, E. S. Gorshina, T. V. Rusinova, V. A. Serezhenkov, D. S. Burbaev, I. G. Gazaryan and A. I. Yaropolov, *Biochimie*, 2004, **86**, 693–703.
20 M. L. Mena, V. Carralero, A. Gonzalez-Cortes, P. Yanez-Sedeno and J. M. Pingarron, *Electroanalysis*, 2005, **17**, 2147–2155.
21 Y. Xiao, F. Patolsky, E. Katz, J. F. Hainfeld and I. Willner, *Science*, 2003, **299**, 1877–1881.
22 A. E. Palmer, S. K. Lee and E. I. Solomon, *J. Am. Chem. Soc.*, 2001, **123**, 6591–6599.
23 G. L. Simpson and B. J. Ortwerth, *Biochim. Biophys. Acta*, 2000, **1501**, 12–24.
24 A. Ramanavicienea, G. Nastajute, V. Snitka, A. Kausaitea, N. German, D. Barauskas-Memenas and A. Ramanavicius, *Sens. Actuators, B*, 2009, **137**, 483–489.
25 E. Akyilmaz and E. Dinckaya, *Talanta*, 1999, **50**, 87–93.
26 M. Liu, Y. P. Wen, J. K. Xu, H. H. He, D. Li, R. R. Yue and G. D. Liu, *Anal. Chem.*, 2011, **27**, 477–482.
27 X. Y. Wang, H. Watanabe and S. Uchiyama, *Talanta*, 2008, **74**, 1681–1685.
28 J. B. He, G. P. Jin, Q. Z. Chen and Y. Wang, *Anal. Chim. Acta*, 2007, **585**, 337–343.

29 I. Kubo, Y. Nakane and N. Maehara, *Electrochim. Acta*, 2006, **51**, 5163–5168.
30 Z. Wang, Q. Xu, J. H. Wang, Q. Yang, J. H. Yu and Y. D. Zhao, *Microchim. Acta*, 2009, **165**, 387–392.
31 B. Hvolbak, T. V. W. Janssens, B. S. Clausen, H. Falsig, C. H. Christensen and J. K. Norskov, *Nano Today*, 2007, **2**, 14–18.
32 M. Haruta and M. Daté, *Appl. Catal., A*, 2001, **222**, 427–437.
33 K. Ramachandran, T. R. kumar, K. J. Babu and G. G. kumar, *Sci. Rep.*, 2016, **6**, 36583–36613.